
ТЕХНІКА ТА МЕТОДИ ЕКСПЕРИМЕНТУ

ENGINEERING AND METHODS OF EXPERIMENT

УДК 615.849+612.014.48

<https://doi.org/10.15407/jnpae2024.04.388>**Bilalodin^{1*}, A. Haryadi¹, Sehad¹, Zufahair², Y. Sardjono³, R. Tursinah⁴**¹ *Department of Physics, Faculty of Mathematics and Natural Science, Jenderal Soedirman University, Purwokerto, Java, Indonesia*² *Department of Chemistry, Faculty of Mathematics and Natural Science, Jenderal Soedirman University, Purwokerto, Java, Indonesia*³ *Research Centre for Accelerator Technology, National Research and Innovation Agency, Jakarta, Indonesia*⁴ *Center for Applied Nuclear Science and Nuclear Agency, Bandung, Indonesia*

*Corresponding author: bilalodin@unsoed.ac.id

**MICRODOSIMETRY TEST ON DOUBLE LAYER BEAM
SHAPING ASSEMBLY NEUTRON BEAM AS A BORON NEUTRON CAPTURE
THERAPY NEUTRON SOURCE USING PHITS CODE**

A microdosimetry test on a double layer beam shaping assembly (DLBSA) neutron beam has been carried out using the particle and heavy ion transport code system (PHITS). The test aims to understand the mechanism of interactions between neutrons and microcells and to determine the linear energy transfer (LET) and the relative biological effectiveness (RBE) values of the DLBSA neutron beam. The test was carried out by interacting a neutron beam with microcells containing ¹⁰B using a boron concentration of 70 ppm. The neutron source used comes from a 30 MeV cyclotron-based DLBSA. The simulation results show that the interaction of neutrons with microcells occurs through scattering, reflection, and absorption reaction mechanisms. The results of the microdosimetry test showed that the peak LET value of α -particles was 100 keV/ μ m and ⁷Li was 200 keV/ μ m, with an RBE value for α of 9.83 and ⁷Li of 6.11.

Keywords: microdosimetry, microcell, linear energy transfer, relative biological effectiveness, particle and heavy ion transport code system, boron neutron capture therapy.

1. Introduction

Boron neutron capture therapy (BNCT) is a therapy method for destroying cancer cells by shooting neutrons at them. The key to successful cancer therapy using the BNCT method is determined by two factors, which include the accumulation of ¹⁰B in cancer cells and the availability of a neutron source that meets BNCT criteria [1, 2].

The source of neutrons can be nuclear reactors, radioisotopes, and accelerators. One type of accelerator that is being developed is the cyclotron [3, 4]. The neutron beams produced from the cyclotron cannot be used directly for BNCT because they still consist of fast neutrons and contain many contaminants [5]. Therefore, they need to be processed using a beam shaping assembly (BSA) to obtain an output neutron beam from the BSA with characteristics that agree with the International Atomic Energy Agency (IAEA) standards. The standard for neutron beams is set as the requirement for BNCT.

One of the BSA designs that is developed to meet the IAEA standards is the double layer beam shaping assembly (DLBSA) model. The BSA design can produce neutron flux according to IAEA standards. The neutron beam from DLBSA has been tested on head, lung, and thyroid cancer cells. The

test is intended to obtain the most effective boron concentration that results in the maximum therapeutic dose. A simulation result showed that neutrons from DLBSA reach the maximum dose of BNCT and a therapy time of less than 1 hour on head, lung, and thyroid tumors at a boron concentration of 60 - 70 ppm [6].

The neutron beam from DLBSA is subjected to a microdosimetry test. This test is crucial to determine the quality of neutron radiation at the cellular level [7]. The quality of neutron radiation is indicated by parameters such as linear energy transfer (LET) and relative biological effectiveness (RBE) [8]. LET refers to the average amount of energy transferred to the medium through which radiation source particles travel per unit distance, expressed in a unit of keV/ μ m [9]. As for RBE, it shows the level of damage to cells due to radiation exposure. Microdosimetry testing is also significant to determine the most effective location to place ¹⁰B in cancer cells, whether in the cell nucleus or the cell wall. Effective location determination is essential in developing boron carrier compounds, which deliver ¹⁰B to cancer cells [7, 10].

Neutron beam microdosimetry tests have been carried out by Lund et al. [11]. Running a test on mono-energy neutrons exposed to body tissue cells,

they concluded that the RBE value is highly dependent on the energy of the neutrons that interact with body tissue cells. Fukunaga et al. [12] ran a simulation of tumor cells, with and without ^{10}B in them, that are irradiated by thermal neutrons. Their result shows that cells containing boron absorb neutrons more effectively than those without boron. Hu et al. [13] carried out a microdosimetry test on thermal neutron beams produced by the Kyoto University Research Reactor (KUR) using a tissue equivalent proportional counter containing boron of 20–100 ppm. Their results showed that the neutron radiation from KUR produced an RBE of 4.2 to 4.4 and a LET value of $100 \text{ keV}/\mu\text{m}$. According to Hariguchi et al. [14], a simulation dosimetry test can also use a water phantom.

Microdosimetry tests are carried out experimentally and by simulation. A simulation approach typically uses a Monte Carlo-based program. The Monte Carlo method is an excellent technique for understanding the mechanisms of radiation effects at

the cellular level [15]. One of the Monte Carlo-based software currently being developed is the particle and heavy ion transport code system (PHITS). This software has been successfully developed to support medical research [16]. In this work, a microdosimetry test will be carried out on neutron beams produced by the DLBSA system on microcells in a water phantom using a boron concentration of 70 ppm.

2. Materials and methodology

2.1. Model of cell in the water phantom

The cell model used in the microdosimetry test is spherical with a cell membrane radius $r_{\text{cell}} = 5 \mu\text{m}$ and a core radius $r_{\text{nuc}} = 2.5 \mu\text{m}$ [17]. The number of cells used in the test is $11 \times 11 \times 11$ cells. The cells were placed in a $15 \times 15 \times 15 \text{ cm}^3$ water phantom at the position (0,0,1.5) cm in front of the neutron beam output from the DLBSA. The multicell model in the water phantom is shown in Fig. 1, *a*.

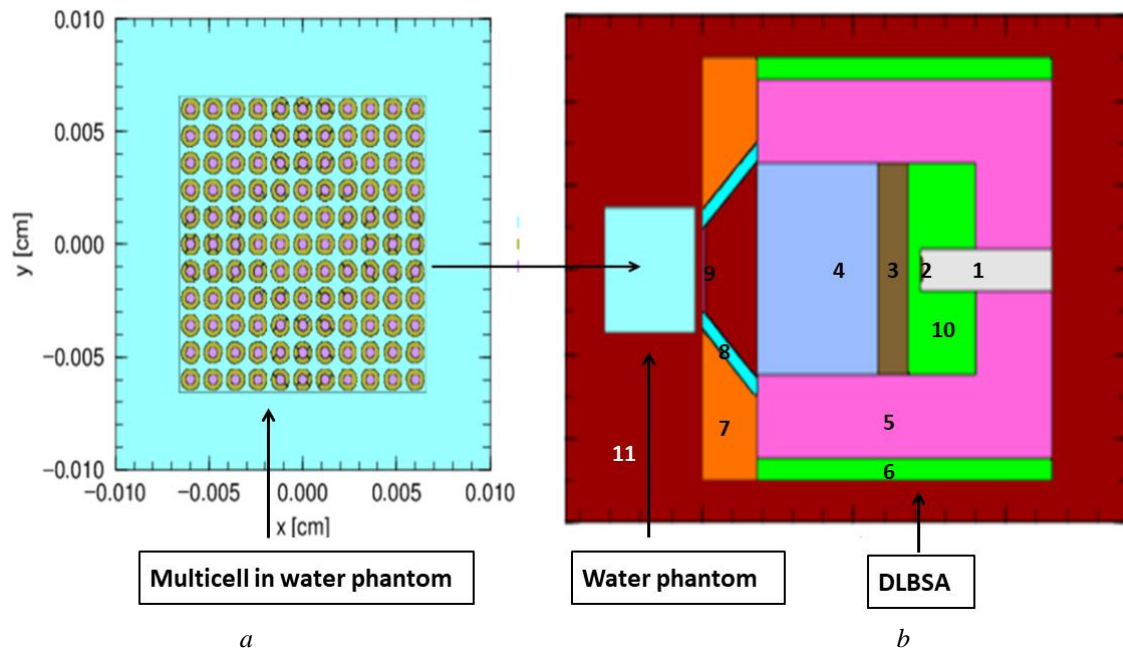


Fig. 1. Schematic diagram of the neutron beam microdosimetry test from DLBSA using an $11 \times 11 \times 11$ multicell. *a* – The water phantom is represented by a blue rectangle and the multicells are small brown circles; *b* – the DLBSA components consist of a moderator in dark brown (3) and pastel blue (4), a reflector in magenta (5) and green (6), a collimator in orange (7) and cyan (8), and a filter in brown (9) and green (10). Meanwhile, the proton channel with an energy of 30 MeV is shown in white (1), while the Be target is depicted in black (2). Outside the DLBSA, the air is represented in winered (11). (See color Figure on the journal website.)

2.2. Neutron source

The source of neutrons is a 30 MeV cyclotron, which is processed using a DLBSA system. The neutrons originating from the DLBSA are generated from the interactions of 30 MeV protons with the beryllium target. The DLBSA is modeled with four main components: a moderator, a reflector, a collimator, and a filter. Each component is made from a

combination of two materials. The moderator is composed of aluminum and BiF_3 . The reflector is made from a combination of lead and carbon. The collimator consists of nickel and borated polyethylene. A combination of iron and cadmium is used as filters for fast and thermal neutrons. The DLBSA model is shown in Fig. 1, *b*.

The characteristics of the neutrons are epithermal neutron flux of $1.1 \times 10^9 \text{ n}/\text{cm}^2 \cdot \text{s}$, the ratio of epi-

thermal neutron flux and thermal neutron flux of 344, ratio of epithermal neutron flux and fast neutron flux of 85, ratio of fast-neutron dose rate and epithermal flux of $1.09 \times 10^{-13} \text{ Gy}\cdot\text{cm}^2$, and the ratio of gamma dose rate and epithermal neutron flux of $1.82 \times 10^{-13} \text{ Gy}\cdot\text{cm}^2$ [18].

2.3. Calculation of LET

The quality of the neutron beam is evaluated by its LET calculations. It is determined through simulation using the PHITS version 2.88 [19]. Visualization of the interactions between thermal neutrons and the water phantom and cells in the water phantom can be created using the Tally Track, and the LET value is determined using the Tally LET [20]. The values of LET are determined solely on α and lithium particles, which result from the decay of thermal neutron interactions with ^{10}B in the cell.

2.4. Calculation of RBE

The RBE value is determined based on Eq. (1) [13].

$$RBE = \int_{-\infty}^{\infty} r(y) \cdot d(y) \cdot dy, \quad (1)$$

where $d(y)$ is the probability distribution of linear energy or dose distribution, y is the LET value, and $r(y)$ is a function of biological response to the radiation. Types of radiation with low LET values have a fixed value of $r(y) = 1$, while those with high LET will have fluctuating $r(y)$ values. The $r(y)$ for this study was estimated using a 2 Gy biological response of fractional cell survival [21].

3. Results and discussions

3.1. Modeling of ^{10}B -filled microcells in the water phantom

The cell model is a ball with a cell nucleus of radius $2.5 \mu\text{m}$ and a cell membrane of radius $5 \mu\text{m}$. The cells filled with ^{10}B with a concentration of 70 ppm are located in the cell nucleus in the water phantom. The microcell was placed 1.5 cm from the wall of the water phantom and 1 cm from the outlet tip of the DLBSA. The results of the interaction of neutron particles from DLBSA with a water phantom containing ^{10}B -filled microcells are shown in Fig. 2.

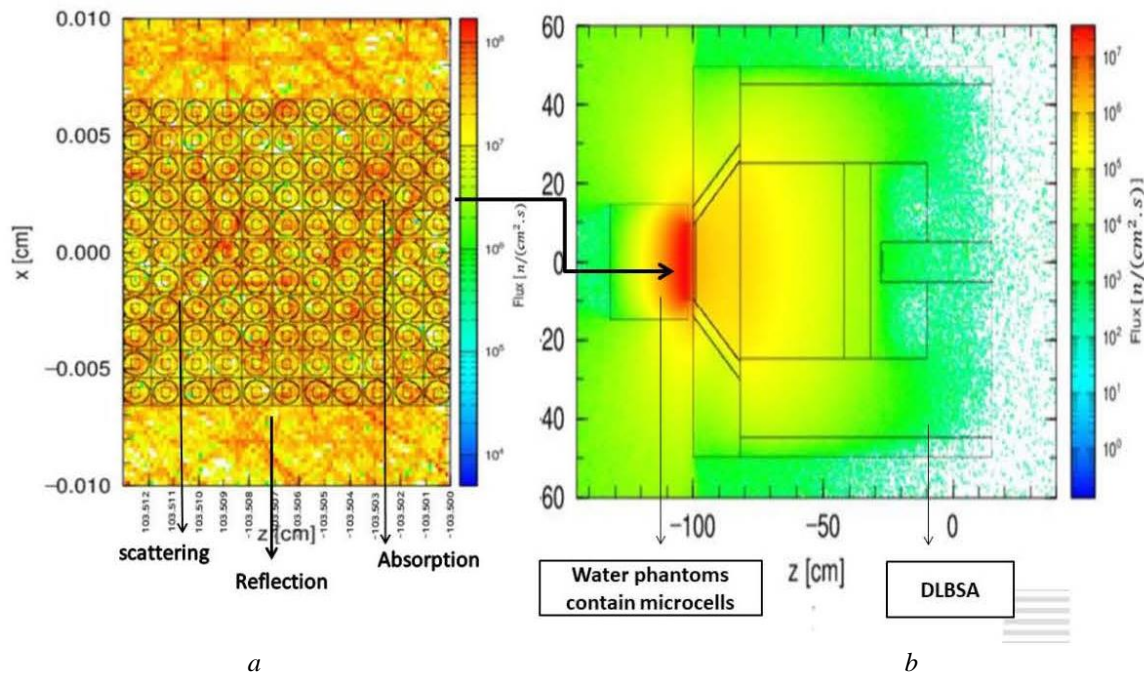


Fig. 2. *a* – Interaction of the neutron beam from DLBSA with the water phantom; *b* – visualization of the interaction of neutrons from DLBSA with microcells in a water phantom. (See color Figure on the journal website.)

The intensity of the neutron flux from DLBSA striking the water phantom containing microcells is expressed in color. The highest neutron flux is shown in red, and the lowest in blue. Fig. 2 shows that the highest neutron flux intensity occurs around the output end of the DLBSA and the water phantom. It suggests that neutron interactions primarily occur in the water phantom. These neutrons also interact with ^{10}B -filled microcells.

The visualization results of the interaction of neutron flux with ^{10}B -filled microcells show that the interaction of neutrons with microcells occurs through scattering, reflection, and absorption reaction mechanisms [22]. The scattering reaction occurs when the direction of the neutrons at an angle collides with the microcells (forming a color trail that passes between the microcells). The reflection reaction occurs when the direction of the neutron colli-

ding with the microcell is perpendicular so that the neutron reverses to its original direction. Absorption reactions occur when microcells absorb neutrons and decay and produce α and ${}^7\text{Li}$ particles (the cell nucleus has a red intensity).

The intensity of neutron fluxes in cells varies. It suggests that the number of neutrons absorbed by cells varies, shown by different intensities of color in the cells, some are yellow, and some are red. The difference in the number of neutrons will cause the number of α and lithium particles produced from the interaction of thermal neutrons with ${}^{10}\text{B}$ in the cell to vary as well.

3.2. Calculation of LET and RBE

The LET is the average amount of energy transferred through a medium per unit length. The simu-

lation of calculating the LET value from the interaction of neutrons with microcells produces the LET spectrum of α and ${}^7\text{Li}$, as shown in Fig. 3. The interactions of neutrons with microcells result in a spectrum of α LET, varying from 10^{-6} to $150 \text{ keV}/\mu\text{m}$. Meanwhile, the LET values of ${}^7\text{Li}$ particles range from 10^{-6} to $300 \text{ keV}/\mu\text{m}$. The peak LET values of α and ${}^7\text{Li}$ particles are 100 and $200 \text{ keV}/\mu\text{m}$, respectively. The variation in LET values is probably caused by the neutrons produced by DLBSA having energy variations of 10^{-6} to 1 MeV [18]. The LET values of α and ${}^7\text{Li}$ particles result from the interaction of thermal neutrons with ${}^{10}\text{B}$ in microcells. The LET value is higher than the value obtained by Hu et al. [23].

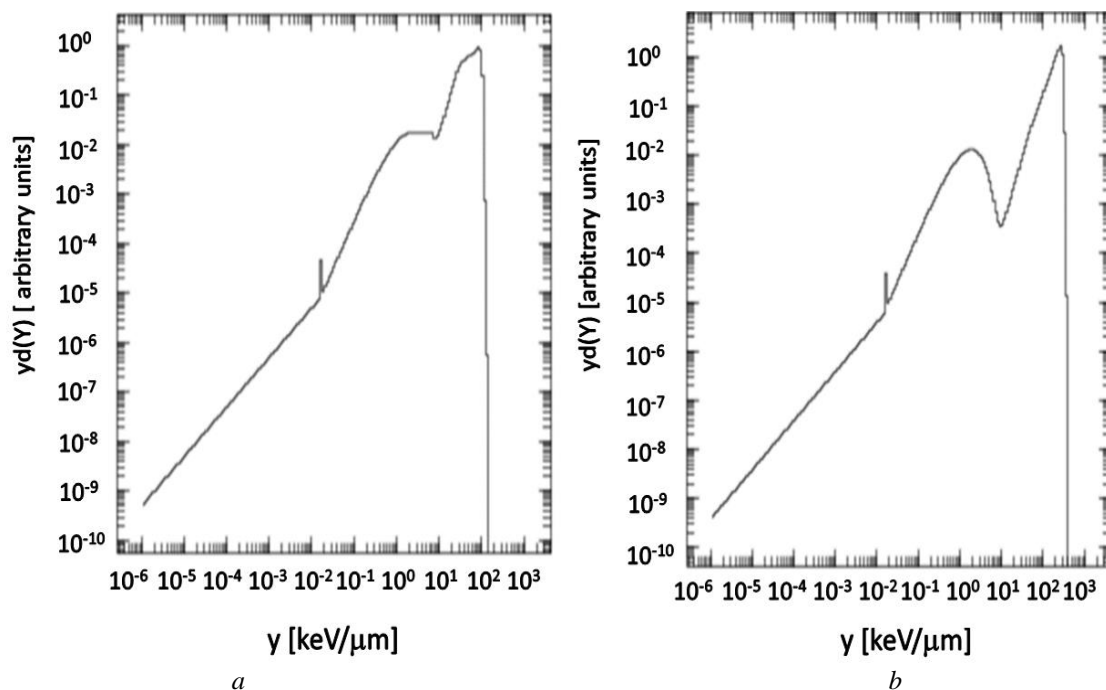


Fig. 3. *a* – Spectrum of α LET; *b* – spectrum of ${}^7\text{Li}$ LET.

The calculation of RBE for α and ${}^7\text{Li}$ particles using Eq. (1) in the energy range of 10^{-6} to $200 \text{ keV}/\mu\text{m}$ results in an RBE value for α particles of 9.83 and an RBE value for ${}^7\text{Li}$ particles of 6.11. The RBE value is higher than the result of Hu et al. [23]. A higher RBE indicates that neutron radiation from DLBSA is more effective in destroying cancer cells than gamma radiation or X-rays. The high RBE value is likely due to the neutron beam produced by DLBSA being epithermal neutrons. Hence, when they enter the phantom water and strike the multi-cell, they turn into high-energy neutrons in the thermal neutron region ($\cong \text{keV}$).

4. Conclusion

The neutron beam microdosimetry test of the DLBSA has been successfully carried out using a

${}^{10}\text{B}$ -containing microcell model in a water phantom using the PHITS code. The microcells are spherical with a cell nucleus radius of $2.5 \mu\text{m}$ and a cell membrane radius of $5 \mu\text{m}$. The neutrons from DLBSA interact with microcells through scattering, reflection, and absorption mechanisms. The LET value produced by the interaction of thermal neutrons with microcells has varying values. The calculation of LET gives the highest LET value for α of $100 \text{ keV}/\mu\text{m}$ and for ${}^7\text{Li}$ of $200 \text{ keV}/\mu\text{m}$. The calculation result of the RBE value for α is 9.83, and for ${}^7\text{Li}$ is 6.11.

The authors express their gratitude to Institutions for Research and Community Service (LPPM) Jenderal Soedirman University which has fully funded this research through the 2023 Unsoed Basic Research Grant.

REFERENCES

1. W.A.G. Sauerwein. Principles and roots of neutron capture therapy. In: W. Sauerwein et al. (Eds.). *Neutron Capture Therapy* (Berlin - Heidelberg: Springer, 2012) p. 1.
2. A.M. Hassanein et al. An optimized epithermal BNCT beam design for research reactors. *Progress in Nuclear Energy* 106 (2018) 455.
3. H. Tanaka et al. Experimental verification of beam characteristics for cyclotron-based epithermal neutron source (C-BENS). *Applied Radiation and Isotopes* 69(12) (2011) 1642.
4. Y. Hashimoto, F. Hiraga, Y. Kiyanagi. Effects of proton energy on optimal moderator system and neutron-induced radioactivity of compact accelerator-driven $^9\text{Be}(p, n)$ neutron sources for BNCT. *Physics Procedia* 60 (2014) 332.
5. S. Hang et al. Monte Carlo study of the beam shaping assembly optimization for providing high epithermal neutron flux for BNCT based on D-T neutron generator. *Journal of Radioanalytical and Nuclear Chemistry* 310(3) (2016) 1289.
6. Bilalodin et al. Optimization and verification of double layer beam shaping assembly (DLBSA) for epithermal neutron generation. *Jurnal Teknologi* 84(4) (2022) 103.
7. J. Vohradsky et al. Evaluation of silicon based microdosimetry for boron neutron capture therapy quality assurance. *Physica Medica* 66 (2019) 8.
8. T. Sato et al. Microdosimetric modeling of biological effectiveness for boron neutron capture therapy considering intra- and intercellular heterogeneity in ^{10}B distribution. *Scientific Reports* 8 (2018) 988.
9. C.B. Sylvester et al. Radiation-induced cardiovascular disease: mechanisms and importance of linear energy transfer. *Frontiers in Cardiovascular Medicine* 5 (2018) 5.
10. R.F. Barth, P. Mi, W. Yang. Boron delivery agents for neutron capture therapy of cancer. *Cancer Communications* 38(1) (2018) 1.
11. C.M. Lund et al. A microdosimetric analysis of the interactions of mono-energetic neutrons with human tissue. *Physica Medica* 73 (2020) 29.
12. H. Fukunaga. Implications of radiation microdosimetry for accelerator-based boron neutron capture therapy: a radiobiological perspective. *The British Journal of Radiology* 93 (2020) 20200311.
13. N. Hu et al. Evaluation of PHITS for microdosimetry in BNCT to support radiobiological research. *Applied Radiation and Isotopes* 161 (2020) 109148.
14. H. Horiguchi et al. Estimation of relative biological effectiveness for boron neutron capture therapy using the PHITS code coupled with a microdosimetric kinetic model. *Journal of Radiation Research* 56(2) (2015) 382.
15. P. Shamshiri, G. Forozani, A. Zabihi. An investigation of the physics mechanism based on DNA damage produced by protons and alpha particles in a realistic DNA model. *Nucl. Instrum. Methods B* 454 (2019) 40.
16. T. Furuta, T. Sato. Medical application of particle and heavy ion transport code system PHITS. *Radiological Physics and Technology* 14(3) (2021) 215.
17. Y. Han et al. Microdosimetric analysis for boron neutron capture therapy via Monte Carlo track structure simulation with modified lithium cross-sections. *Radiation Physics and Chemistry* 209 (2023) 110956.
18. Bilalodin et al. Optimization and analysis of neutron distribution on 30 MeV cyclotron-based double layer beam shaping assembly (DLBSA). *Nucl. Phys. At. Energy* 20 (2019) 70.
19. T. Sato et al. Particle and heavy ion transport code system, PHITS, version 2.52. *Journal of Nuclear Science and Technology* 50(9) (2013) 913.
20. T. Sato et al. Features of particle and heavy ion transport code system (PHITS) version 3.02. *Journal of Nuclear Science and Technology* 55(6) (2018) 684.
21. A. Tilikidis et al. An estimation of the relative biological effectiveness of 50 MV bremsstrahlung beams by microdosimetric techniques. *Physics in Medicine & Biology* 41(1) (1996) 55.
22. I.S. Anderson et al. Research opportunities with compact accelerator-driven neutron sources. *Physics Reports* 654 (2016) 1.
23. N. Hu et al. Microdosimetric quantities of an accelerator-based neutron source used for boron neutron capture therapy measured using a gas-filled proportional counter. *Journal of Radiation Research* 61(2) (2020) 214.

Біلالодін^{1,*}, А. Хар'яді¹, Сехах¹, Зусфахайр², Ю. Сарджоно³, Р. Турсіна⁴

¹ Кафедра фізики, факультет математики та природничих наук, Університет Джендерала Содірмана, Пурвокерто, Ява, Індонезія

² Кафедра хімії, факультет математики та природничих наук, Університет Джендерала Содірмана, Пурвокерто, Ява, Індонезія

³ Дослідницький центр прискорювальних технологій,

Національне агентство з досліджень та інновацій, Джакарта, Індонезія

⁴ Центр прикладної ядерної науки та Агентство ядерної енергії, Бандунг, Індонезія

*Відповідальний автор: bilalodin@unsoed.ac.id

МІКРОДОЗИМЕТРИЧНИЙ ТЕСТ ДВОШАРОВОГО БЛОКА ФОРМУВАННЯ НЕЙТРОННОГО ПУЧКА ЯК ДЖЕРЕЛА ДЛЯ НЕЙТРОННОЇ ТЕРАПІЇ ІЗ ЗАХОПЛЕННЯМ БОРНИХ НЕЙТРОНІВ З ВИКОРИСТАННЯМ ПРОГРАМИ PHITS

Мікродозиметричний тест двошарового блока формування нейтронного пучка (DLBSA) було проведено за допомогою програми розрахунку переносу частинок і важких іонів (PHITS). Тест має на меті прояснити

механізм взаємодії між нейтронами та мікроклітинами та визначити значення лінійної передачі енергії (LET) і відносної біологічної ефективності (RBE) пучка нейтронів DLBSA. Тест проводили для пучка нейтронів з мікроклітинами, що містять ^{10}B , з використанням концентрації бору 70 ppm. Використане джерело нейтронів походить від DLBSA на основі циклотрона з енергією 30 МеВ. Взаємодія нейтронів з мікроклітинами відбувається через реакції розсіювання, відбиття та поглинання. Результати мікродозиметричного тесту показали, що пікове значення LET для α -частинок становило 100 кеВ/мкм, а для ^7Li – 200 кеВ/мкм, зі значенням RBE для α 9,83 і ^7Li – 6,11.

Ключові слова: мікродозиметрія, мікроклітини, лінійна передача енергії, відносна біологічна ефективність, програма моделювання транспорту частинок і важких іонів, терапія із захопленням борних нейтронів.

Надійшла / Received 15.02.2024